Estrogen receptor-α signaling in osteoblast progenitors stimulates cortical bone accrual

Maria Almeida, Srividhya Iyer, Marta Martin-Millan, Shoshana M. Bartell, Li Han, Elena Ambrogini, Melda Onal, Jinhu Xiong, Robert S. Weinstein, Robert L. Jilka, Charles A. O'Brien, and Stavros C. Manolagas

Division of Endocrinology and Metabolism, Center for Osteoporosis and Metabolic Bone Diseases, University of Arkansas for Medical Sciences and Central Arkansas Veterans Healthcare System, Little Rock, Arkansas, USA.

The detection of estrogen receptor-α (ERα) in osteoblasts and osteoclasts over 20 years ago suggested that direct effects of estrogens on both of these cell types are responsible for their beneficial effects on the skeleton, but the role of ERα in osteoblast lineage cells has remained elusive. In addition, estrogen activation of ERα in osteoclasts can only account for the protective effect of estrogens on the cancellous, but not the cortical, bone compartment that represents 80% of the entire skeleton. Here, we deleted *ER*α at different stages of differentiation in murine osteoblast lineage cells. We found that ERα in osteoblast progenitors expressing Osterix1 (Osx1) potentiates Wnt/β-catenin signaling, thereby increasing proliferation and differentiation of periosteal cells. Further, this signaling pathway was required for optimal cortical bone accrual at the periosteum in mice. Notably, this function did not require estrogens. The osteoblast progenitor *ER*α mediated a protective effect of estrogens against endocortical, but not cancellous, bone resorption. ERα in mature osteoblasts or osteocytes did not influence cancellous or cortical bone mass. Hence, the ERα in both osteoblast progenitors and osteoclasts functions to optimize bone mass but at distinct bone compartments and in response to different cues.

Introduction

The volume of bone mass is determined by the balance between two opposing processes, bone removal (resorption) by osteoclasts and bone formation by osteoblasts. Under physiologic circumstances, formation compensates for the effect of resorption by adding bone either in the same anatomical site from which it was previously resorbed, in a process called remodeling, or in a different site, as in the case of the sculpting of bones during growth, in a process called modeling (1).

After birth, long bones in both sexes increase in length. In parallel with linear growth, females and males experience an enlargement and thickening of the bone cortex, because bone apposition at the periosteal (outer) envelope exceeds the widening of the medullar cavity by endocortical resorption. Importantly, with the onset of puberty, estrogens inhibit, while androgens stimulate, periosteal bone formation, thereby contributing to sexual dimorphism and the greater bone mass in the male (2). At the same time, endocortical resorption is attenuated by either estrogens or androgens, producing increased cortical thickness at the end of puberty in both sexes. In line with the inhibitory effect of estrogens on periosteal bone formation, estrogen deficiency in female rodents and postmenopausal women increases periosteal apposition in an attempt to compensate for the endocortical loss of bone. At the end of puberty, estrogens are essential for the closure of the epiphyses and the cessation of linear growth (3).

Estrogens also slow the rate of bone remodeling and help to maintain a balance between bone formation and resorption by attenuating the birth rate of osteoclast and osteoblast progenitors in the bone marrow and exerting a proapoptotic effect on osteoclasts and an antiapoptotic effect on osteoblasts and osteocytes (4–6). Conversely, estrogen deficiency causes an increase in bone remodeling, increased osteoclastogenesis and osteoblastogenesis, increased osteoclast and osteoblast numbers, and increased resorption and formation although these are unbalanced. Heretofore, however, it remains unknown whether estrogens exert their positive influence on bone exclusively through their well-established antiresorptive actions or have additional bone-forming effects.

Recently, we and others have shown that selective deletion of the estrogen receptor-α (*ER*α) from cells of the osteoclast lineage increases osteoclastogenesis, abrogates the effects of estrogens on osteoclast apoptosis, increases bone resorption in the female but not the male, and causes loss of cancellous bone (7, 8). However, *ER*α deletion from osteoclasts does not affect cortical bone, raising the possibility that effects of estrogens on other cell types may be responsible for their effects on cortical bone.

Here, we have determined the role of ERα in osteoblastic cells by deleting it at different stages of osteoblast differentiation. We report that, in sharp contrast to the inhibitory effect of estrogens on periosteal bone expansion, the unliganded ERα present in osteoblast precursors stimulates bone formation in the periosteum by potentiating Wnt/T cell factor–mediated (Wnt/TCF-mediated) transcription. In addition, the osteoblast progenitor ERα mediates an indirect inhibitory effect of estrogens on endocortical, but not cancellous, bone resorption.

Results

Generation of ERα$^{f/f}$;Prx1-cre mice. To elucidate the biologic role of the ERα in cells of the osteoblast lineage, we crossed mice harboring a floxed *ER*α allele (*ERα$^{f/f}$* mice) (7) with mice expressing the Cre recombinase under the control of regulatory elements of the *Prx1* gene, which is expressed in pluripotent mesenchymal progenitors of the appendicular, but not the axial, skeleton and their progeny (9). The *Prx1-cre* transgene activates a reporter gene

Conflict of interest: Stavros C. Manolagas serves on the scientific advisory board of Radius Health Inc. He has ownership of equity in this company and receives $10,000 per annum for his scientific advisory board service.

Citation for this article: *J Clin Invest.* 2013;123(1):394–404. doi:10.1172/JCI65910.

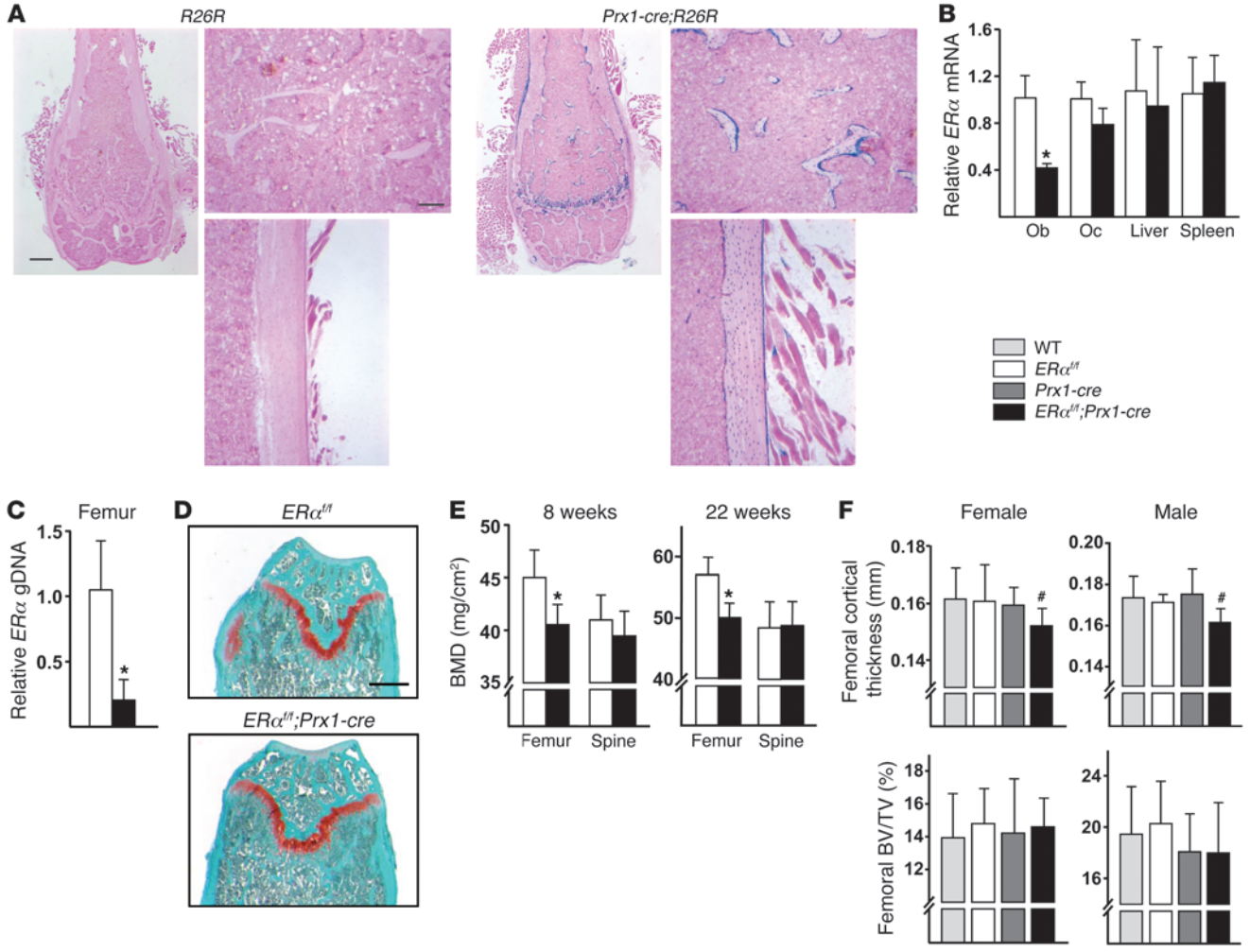

Figure 1

Deletion of *ERα* in *Prx1-cre*–expressing cells decreases cortical bone mass. (**A**) X-gal–stained histological frozen sections of the distal femurs of 24-week-old *R26R* control and *Prx1-cre;R26R* mice. The left panels show a low-magnification image of the distal femur. Scale bar: 500 μm. The right panels show a high-magnification image of the cancellous (top) and cortical bone (bottom). Scale bar: 100 μm. (**B**) *ERα* mRNA levels in cultured osteoblasts (Ob) and osteoclasts (Oc) (6 wells) and livers and spleens (n = 7–9/group). (**C**) Quantitative PCR of loxP-flanked genomic DNA (gDNA), normalized to a control locus, isolated from collagenase-digested femurs and tibia cortical bone (n = 5–7/group). (**D**) Safranin-O–stained histological sections of the distal femurs of 12-week-old mice (cartilage stains red). Scale bar: 500 μm. (**E**) BMDs determined by DEXA in female mice at 8 (n = 9–11/group) and 22 (n = 10/group) weeks of age. (**F**) Cortical thickness determined at the midshaft and cancellous bone volume measured at the distal end by micro-CT in femurs from 8-week-old female (n = 9–11/group) and male mice (n = 6–12/group). BV/TV, bone volume per tissue volume. Bars represent mean and SD. $^*P < 0.05$ by Student's t test; $^{\#}P < 0.05$ versus wild-type, *ERα*$^{f/f}$, and *Prx1-cre* mice by 2-way ANOVA.

(*R26R*) in all the osteoblasts and osteocytes present in cortical and cancellous bone as well as growth plate chondrocytes, at least up to 5 weeks of age (10). Here, we established that *Prx1-cre*–mediated recombination was maintained in all these cell types up to at least 28 weeks of age (Figure 1A), which is the oldest age of mice examined in the studies reported herein. The effectiveness of *ERα* gene deletion was demonstrated by a 60%–80% decrease in *ERα* mRNA levels from cultured osteoblastic cells (Figure 1B) and in *ERα* genomic DNA from femoral shafts (Figure 1C) of *ERα*$^{f/f}$*;Prx1-cre* mice. *ERα* mRNA expression in osteoclasts, livers, and spleens was unaffected (Figure 1B). Total body weight, femoral length (Supplemental Table 1; supplemental material available online with this article; doi:10.1172/JCI65910DS1), and the morphology of the growth plate (Figure 1D) were also unaffected by *ERα* deletion in *Prx1-cre*–expressing cells. Likewise, *ERα*$^{f/f}$*;Prx1-cre* mice had normal uterine weight, indicating that estrogen levels were not affected (Supplemental Table 1).

ERα$^{f/f}$*;Prx1-cre mice have low femoral bone mass.* Female *ERα*$^{f/f}$*;Prx1-cre* mice exhibited low bone mineral density (BMD) in the femur up to at least 22 weeks of age, as determined by dual-energy x-ray absorptiometry (DEXA), compared with *ERα*$^{f/f}$ littermates (Figure 1E). In line with the fact that the *Prx1-cre* transgene is not expressed in the axial skeleton, spinal BMD was unaltered, providing additional evidence for the specificity of the *ERα* deletion. Micro-CT analysis revealed that the low femoral BMD resulted from decreased cortical thickness but no change in cancellous bone mass (Figure 1F). Albeit, trabecular number was reduced and trabecular spacing was increased in the *ERα*$^{f/f}$*;Prx1-cre* mice at

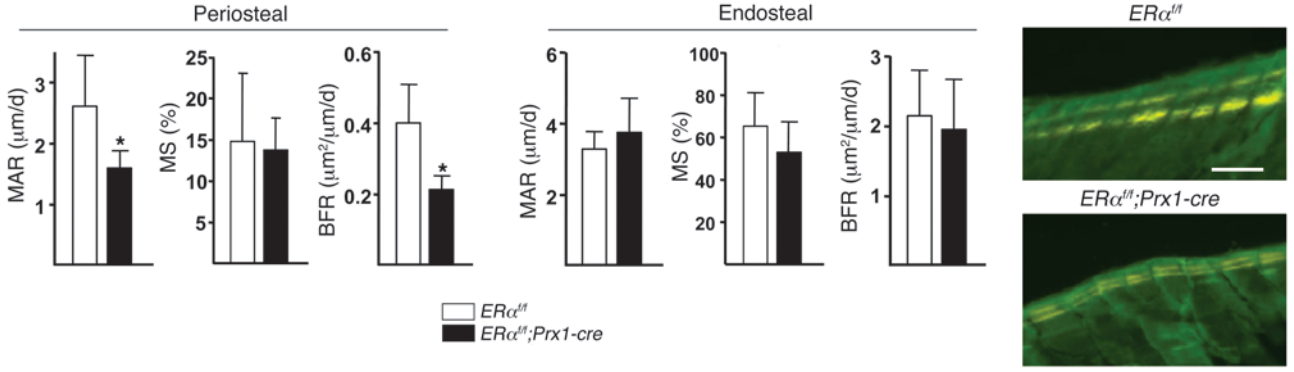

Figure 2
ERα$^{f/f}$;Prx1-cre mice have decreased periosteal bone formation. MAR, MS, and BFR, as determined by tetracycline labels, shown in the photomicrographs (scale bar: 20 μm), in longitudinal undecalcified sections of femurs from 8-week-old female mice (n = 6–7/group). Bars represent mean and SD. *P < 0.05 by Student's t test.

12 weeks of age (Supplemental Table 1). As with the femoral BMD, the decrease in cortical thickness was present up to 28 weeks of age. Similar to that of the females, male *ERα$^{f/f}$;Prx1-cre* mice had decreased cortical thickness but normal cancellous bone mass, as determined at 6 weeks of age (Supplemental Figure 1A) or 8 weeks of age (Figure 1F). Nonetheless, in contrast to that in the females, the cortical decrement was no longer present in 18-week-old *ERα$^{f/f}$;Prx1-cre* male mice (Supplemental Figure 1B).

In agreement with the imaging studies, dynamic histomorphometric analysis of femoral bone sections from 8-week-old *ERα$^{f/f}$;Prx1-cre* females revealed a 40% decrease in mineral apposition rate (MAR) with no change in mineralizing surface (MS), resulting in an overall 50% decrease in bone formation rate (BFR) at the periosteal surface, as compared with the control littermates (Figure 2). However, there was no change in any of the parameters at the endocortical surface. Moreover, consistent with the lack of an effect of *ERα* deletion on cancellous bone mass, the number of osteoblasts and osteoclasts as well as dynamic measures of bone formation were unaffected in the cancellous bone of *ERα$^{f/f}$;Prx1-cre* mice (Supplemental Figure 2, A and B). The number as well as the size of the adipocytes in the bone marrow was unaffected in the *ERα$^{f/f}$;Prx1-cre* mice at 12 weeks of age (Supplemental Figure 2C).

Deletion of ERα from Osterix1-cre–expressing cells recapitulates the skeletal phenotype of the ERα$^{f/f}$;Prx1-cre mice. The skeletal phenotype of the *ERα$^{f/f}$;Prx1-cre* mice could be the result of the loss of receptor function in a pluripotent uncommitted mesenchymal progen-

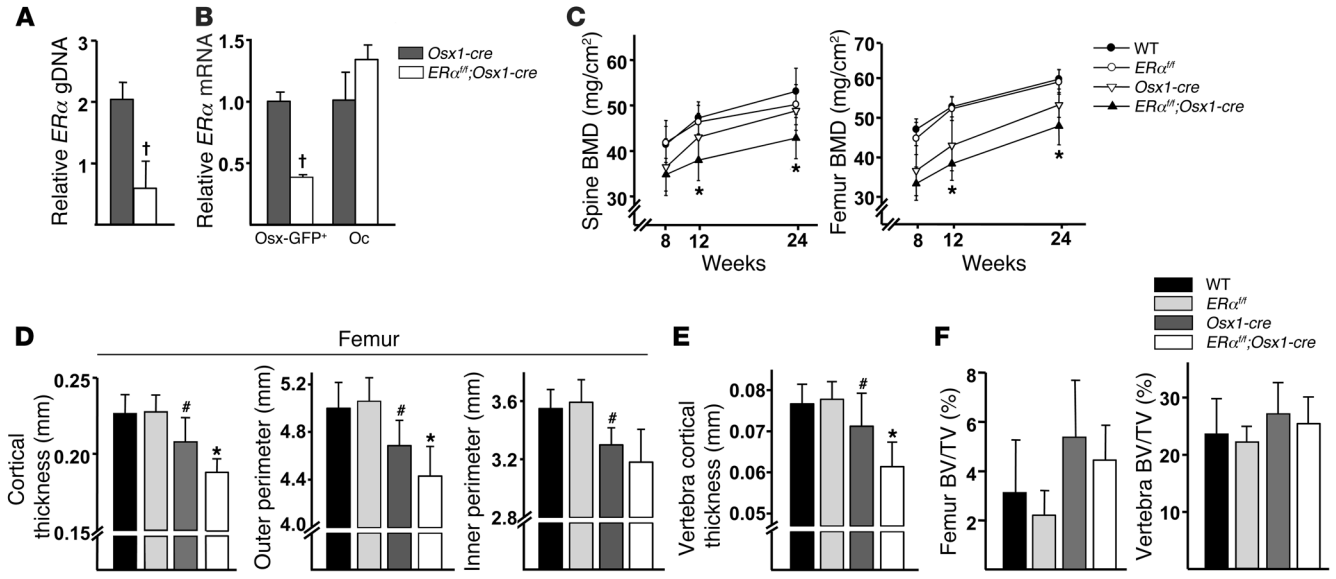

Figure 3
Deletion of ERα in *Osx1-cre*–expressing cells decreases cortical bone mass. (**A**) Quantitative PCR of loxP-flanked genomic DNA, normalized to a control locus, isolated from collagenase-digested femur and tibia cortical bone (n = 4–6/group). (**B**) *ERα* mRNA levels by quantitative PCR in cultured Osx1-GFP–positive cells and osteoclasts (triplicate cultures). (**C**) Longitudinal BMD determined by DEXA in female mice (n = 6–11/group). (**D**) Cortical bone measurements determined by micro-CT in the midshaft region of femurs and (**E**) in the fifth lumbar vertebra of 24-week-old mice described in **C**. (**F**) Cancellous bone mass determined by micro-CT in the distal end of the femurs and the fifth lumbar vertebrae of mice described in **D**. Bars represent mean and SD. †P < 0.05 by Student's t test; *P < 0.05 versus *Osx1-cre*; #P < 0.05 versus wild-type or *ERα$^{f/f}$* by 2-way ANOVA.

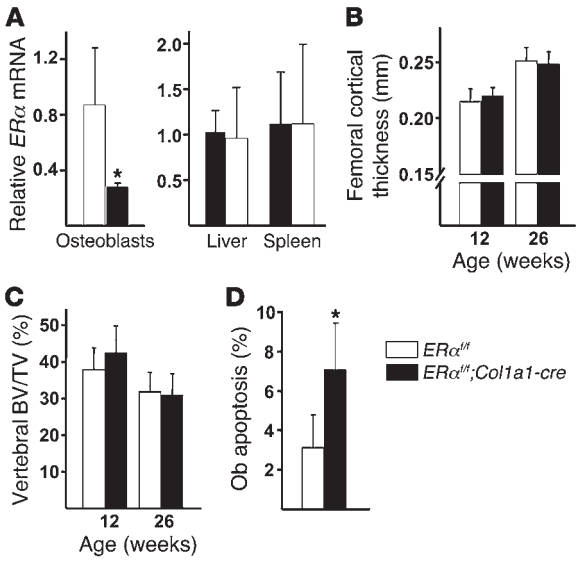

Figure 4
Deletion of ERα in *Col1a1-cre*–expressing cells does not alter bone mass. (**A**) *ERα* mRNA levels in cultured osteoblasts (triplicate wells), liver, and spleen (n = 6/group). (**B**) Cortical thickness measured by micro-CT at the midshaft of the femurs of 12-week-old (n = 11–14/group) and 26-week-old (n = 8–11/group) female mice. (**C**) Cancellous bone mass determined by micro-CT in the fifth lumbar vertebra of mice described in **B**. (**D**) Osteoblast apoptosis in undecalcified sections of L1–L4 vertebra, stained by ISEL, from 26-week-old female mice (n = 4/group). Bars represent mean and SD. *$P < 0.05$ by Student's t test.

itor, a descendent osteoblast progenitor, or terminally differentiated osteoblasts and osteocytes. To distinguish between the first and the second of these possibilities, we next generated mice in which the *ERα* was deleted from cells expressing Osterix1 (*Osx1*) using an *Osx1-GFP::cre* deleter strain (11). The *Osx1-GFP::cre* transgene is expressed in osteoblast progenitors residing in the bone-forming regions of the perichondrium and primary spongiosa as well as in hypertrophic chondrocytes. In addition, Osx1/GFP-expressing cells are present in the thin periosteal layer overlaying the cortical bone surface (12).

ERα genomic DNA in femoral shafts of *ERα$^{f/f}$;Osx1-cre* mice was decreased by 70% as compared with that in *Osx1-cre* control mice (Figure 3A). *ERα* mRNA expression in cultured Osx1-GFP–positive calvaria cells isolated by flow cytometry was similarly decreased by 70% (Figure 3B). In contrast, *ERα* mRNA expression in bone marrow–derived osteoclasts was indistinguishable between *ERα$^{f/f}$;Osx1-cre* and the control mice. Body weight in female *Osx1-cre* or *ERα$^{f/f}$;Osx1-cre* mice was lower as compared with that in wild-type or *ERα$^{f/f}$* littermate control mice (Supplemental Figure 3A), as was femoral length (Supplemental Figure 3B). These findings are in line with a previous report showing that the *Osx1-cre* transgene decreases body size (13). The smaller body size and the reduced femoral length in both *Osx1-cre* and *ERα$^{f/f}$;Osx1-cre* mice notwithstanding, these 2 measures were indistinguishable between *Osx1-cre* and *ERα$^{f/f}$;Osx1-cre* mice. This result indicates that, whereas *Osx1-cre* expression in and of itself had an effect, *ERα* deletion per se did not affect body size or femoral length. Nonetheless, spine and femoral BMD was significantly lower in *ERα$^{f/f}$;Osx1-cre* mice when compared with that of *Osx1-cre* mice at 12 or 24 weeks of age (Figure 3C).

In line with the smaller femur size, mice expressing *Osx1-cre* had decreased cortical thickness as well as smaller outer and inner femoral midshaft bone perimeters when compared with wild-type or *ERα$^{f/f}$* littermate controls (Figure 3D). Once again, in spite of the effects of the *Osx1-cre* transgene by itself, cortical thickness was further decreased by *ERα* deletion in *ERα$^{f/f}$;Osx1-cre* mice when compared with *Osx1-cre* control mice at 24 weeks of age. The decrease in cortical thickness in the *ERα$^{f/f}$;Osx1-cre* mice was due to deficient periosteal apposition, as evidenced by a decrease in the outer perimeter of the midshaft, while the inner perimeter was unaffected. Notably, *ERα$^{f/f}$;Osx1-cre* mice also exhibited decreased cortical thickness in the vertebrae (Figure 3E), demonstrating that the cortical bone phenotype caused by the *ERα* deletion was not restricted to long bones. The cancellous bone volume in the femurs or vertebrae of *ERα$^{f/f}$;Osx1-cre* mice, on the other hand, was indistinguishable among wild-type, *ERα$^{f/f}$*, and *Osx1-cre* littermate controls (Figure 3F). Moreover, trabecular number and spacing were unaffected by *ERα* deletion when compared with *Osx1-cre* mice, but trabecular thickness was decreased (Supplemental Figure 3C). Thus, deletion of *ERα* in osteoblast progenitors led to a phenotype similar to that caused by *ERα* deletion from uncommitted mesenchymal progenitors.

Deletion of ERα in osteoblasts and osteocytes does not alter bone mass. Next, we investigated whether the effect of the *ERα* deletion from *Prx1-cre*– or *Osx1-cre*–expressing cells on bone was the result of loss of function in osteoblast precursors as opposed to their differentiated descendants, i.e., mature osteoblasts and osteocytes. To do this, we generated mice in which the *ERα* was deleted from osteoblasts and osteocytes expressing α1(I)-collagen (*Col1a1*) using a *Col1a1-cre* deleter strain (14). The *Col1a1-cre* transgene activated the reporter gene *R26R* in all the osteoblasts and osteocytes present in cortical and cancellous bone, demonstrating extremely high efficiency of cre-mediated recombination in these cell types (Supplemental Figure 4). Bone marrow–derived osteoblasts from *ERα$^{f/f}$;Col1a1-cre* mice exhibited a 70% reduction in *ERα* expression levels (Figure 4A). *ERα* mRNA expression in livers and spleens was unaffected. Deletion of *ERα* from *Col1a1*-expressing cells had no effect on bone mass, as measured by serial DEXA BMD measurements between 4 and 12 weeks of age in the spines and femurs of female and male mice (Supplemental Figure 5). The lack of an effect of the *ERα* deletion in *Col1a1*-expressing cells on cortical thickness (Figure 4B), cancellous bone mass (Figure 4C), and microarchitecture (Supplemental Table 2) was confirmed by micro-CT analysis in 12- and 26-week-old mice. In spite of the absence of an effect on bone mass, *ERα$^{f/f}$;Col1a1-cre* mice did exhibit the anticipated increase in cancellous osteoblast apoptosis (Figure 4D).

Osteoblastogenesis is attenuated in ERα$^{f/f}$;Prx1-cre and ERα$^{f/f}$;Osx1-cre mice. Having established that the *ERα* expressed in osteoblast progenitors, but not mature osteoblasts or osteocytes, was responsible

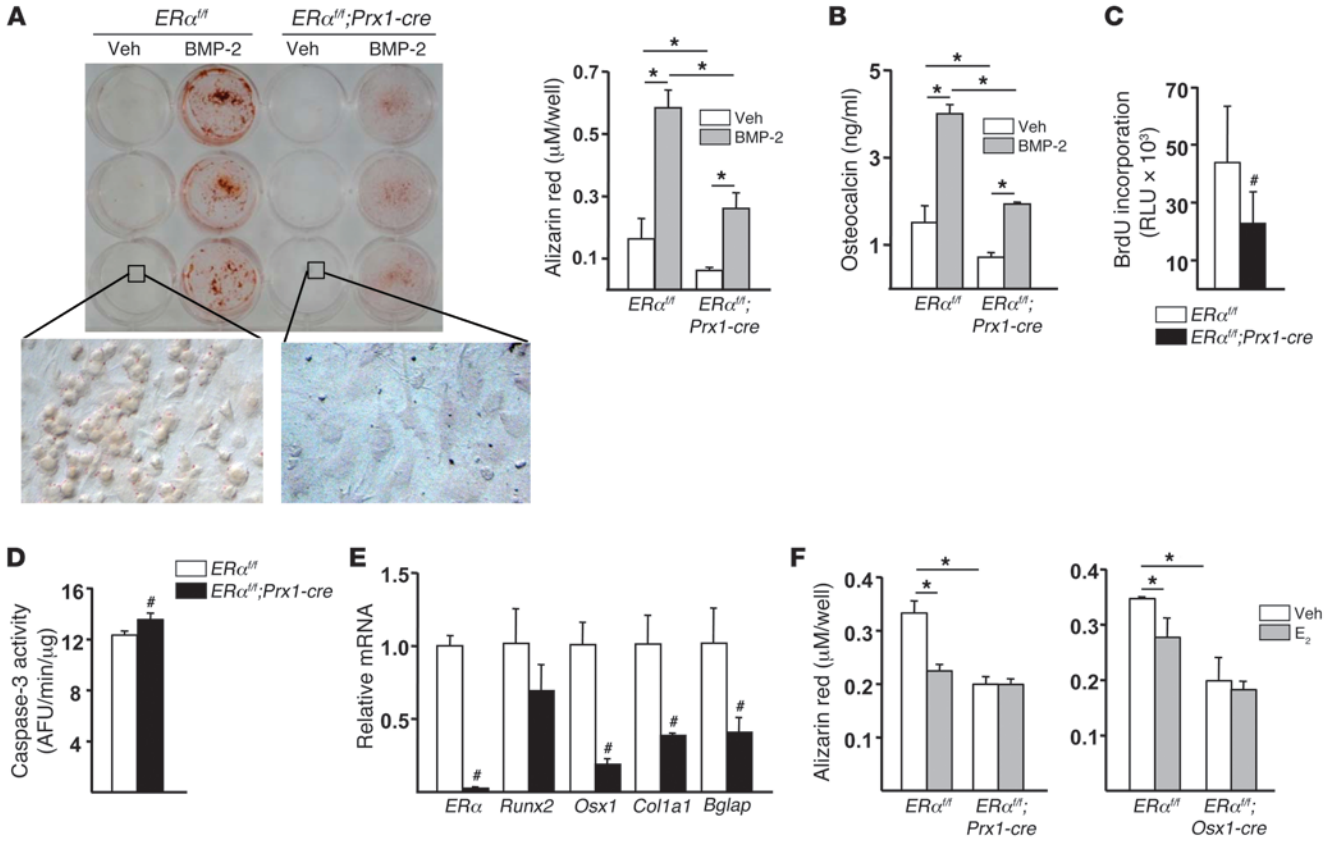

Figure 5

Deletion of ERα decreases proliferation and differentiation of osteoblast progenitors from the periosteum. (**A**) Mineralized matrix visualized and quantified following Alizarin Red staining and (**B**) osteocalcin levels in the medium of periosteal cell cultures pooled from 3 mice treated with vehicle (veh) or rhBMP-2 (25 ng/ml) for 21 days (triplicate cultures). Original magnification, ×63 (bottom row). (**C**) BrdU incorporation and (**D**) caspase-3 activity in periosteal cells cultured for 3 day (6 wells). AFU, arbitrary fluorescence units. (**E**) mRNA levels of the indicated genes determined by quantitative PCR in periosteal cells cultured with ascorbic acid for 14 days (triplicate cultures). (**F**) Mineralized matrix quantified following Alizarin Red staining in periosteal cells cultured with vehicle or E_2 (10^{-8} M) in the presence of ascorbic acid for 21 days (triplicate cultures). Bars represent mean and SD. $^*P < 0.05$ by 2-way ANOVA; $^\#P < 0.05$ by Student's *t* test.

for optimal periosteal bone formation, we went on to investigate the mechanism(s) responsible. To do this, we examined osteoprogenitor proliferation, differentiation, and life span using cultures of periosteal- or bone marrow–derived osteoblastic cells isolated from femurs. In agreement with the decreased periosteal BFR, periosteal cells from *ERα$^{f/f}$;Prx1-cre* mice exhibited a markedly decreased capacity to form mineralized nodules (Figure 5A) and to secrete osteocalcin (Figure 5B), both under basal conditions or in response to BMP-2. These changes were accompanied by a reduction in the number of cells due to a decrease in their proliferation (Figure 5C) and a small increase in apoptosis (Figure 5D). Moreover, the expression of genes involved in osteoblastogenesis, such as *Osx1*, *Col1a1*, and *Bglap* but not *Runx2*, was also decreased in cells from *ERα$^{f/f}$;Prx1-cre* mice as compared with cells from littermate controls (Figure 5E), suggesting that osteoblast differentiation was also affected by the *ERα* deletion in progenitor cells. Similar results were obtained with bone marrow–derived cells (Supplemental Figure 6, A–C).

To establish whether the number of mesenchymal progenitors was affected by the *ERα* deletion, we quantified the number of progenitors able to form CFU-fibroblasts (CFU-F), CFU-osteoblasts (CFU-OB), and CFU-adipocytes (CFU-AD) in ex vivo bone marrow cultures from *ERα$^{f/f}$;Prx1-cre* mice, *ERα$^{f/f}$;Osx1-cre* mice, and their respective control mice. The number of CFU-F, CFU-AD, and CFU-OB was increased in *ERα$^{f/f}$;Prx1-cre* mice compared with that in *ERα$^{f/f}$* control mice (Supplemental Figure 7A). In contrast, the number of CFU-F and CFU-OB in *ERα$^{f/f}$;Osx1-cre* mice was indistinguishable from that in the *Osx1-cre* control mice (Supplemental Figure 7B). As in the case of the *ERα$^{f/f}$;Prx1-cre* mice, the number of CFU-AD was elevated in *ERα$^{f/f}$;Osx1-cre* mice. Interestingly, CFU-OB colonies from *ERα$^{f/f}$;Prx1-cre* and *ERα$^{f/f}$;Osx1-cre* mice were smaller and displayed irregular shapes, consistent with defective osteoblast differentiation.

We have shown earlier that estrogens restrain osteoblastogenesis (15, 16). In agreement with those earlier results, addition of 17β-estradiol to periosteal- (Figure 5F) or bone marrow–derived cell cultures (Supplemental Figure 6D) from control mice had an attenuating effect on osteoblastogenesis, strongly suggesting that the actions of the estrogen-activated ERα are opposite to the ones of the unliganded ERα.

The unliganded ERα potentiates the Wnt/β-catenin signaling pathway. Wnt/β-catenin signaling is essential for osteoblastogenesis, and its

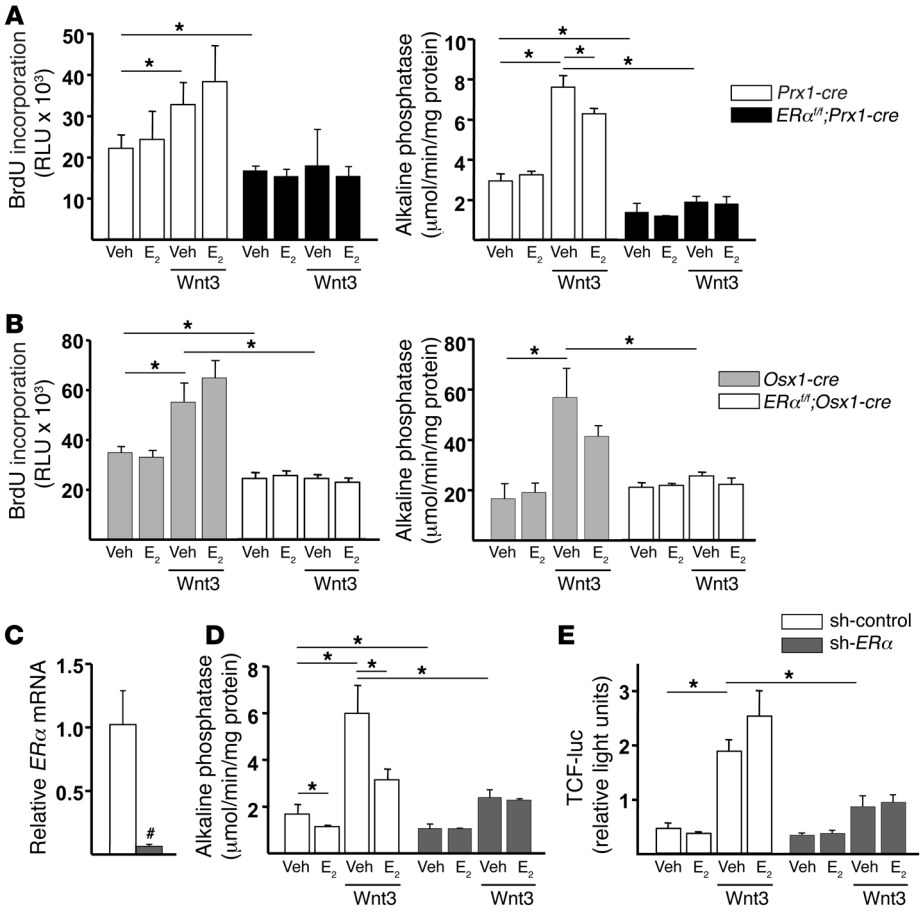

Figure 6
The unliganded *ERα* potentiates the Wnt/β-catenin signaling pathway. BrdU incorporation and AP activity in periosteal cell cultures pooled from 3 mice from each of the (**A**) *ERα$^{f/f}$;Prx1-cre* and *ERα$^{f/f}$* littermate groups and (**B**) the *ERα$^{f/f}$;Osx1-cre* and *Osx1-cre* littermate groups, preincubated for 1 hour with vehicle or E_2 (10^{-8} M), followed by incubation without or with Wnt3 (25 ng/ml) for 3 days. (**C**) *ERα* mRNA levels determined by quantitative PCR in C2C12 cells transduced with lentiviruses encoding a nontarget shRNA (sh-control) or sh-*ERα*. (**D**) AP activity in cells treated as in **A**. (**E**) Luciferase activity in C2C12 cells transfected with a TCF-luc reporter construct and pretreated as in **A**, followed by treatment without or with Wnt3 (12.5 ng/ml) for 24 hours. Bars represent mean and SD. $^*P < 0.05$ by 1-way ANOVA with Bonferroni's test; $^\#P < 0.05$ by Student's *t* test.

effects may be potentiated by ERα (17, 18). In agreement with this evidence, the pro-proliferative and pro-osteoblastogenic actions of Wnt3 were blunted in periosteal cells from *ERα$^{f/f}$;Prx1-cre* (Figure 6A) and *ERα$^{f/f}$;Osx1-cre* mice (Figure 6B). Albeit, 17β-estradiol had no effect on basal or Wnt3-stimulated proliferation and attenuated Wnt3-induced alkaline phosphatase (AP) activity, demonstrating that the effects of the receptor are independent or even opposite to those of its ligand. Practically identical results were obtained with bone marrow–derived cells (Supplemental Figure 8, A and B). To confirm that the effects of ERα on Wnt signaling were independent of estrogens, we silenced *ERα* in C2C12 cells using shRNA directed against *ERα* (sh-*ERα*). Knockdown of *ERα* levels in sh-*ERα* cells was confirmed by quantitative PCR (Figure 6C). Similar to the periosteal cells, Wnt3-induced AP activity was greatly attenuated in sh-*ERα* cells (Figure 6D). In addition, the increase in TCF transcription induced by Wnt3 in nontarget shRNA cells was greatly attenuated in sh-*ERα* cells (Figure 6E). In contrast, 17β-estradiol attenuated Wnt3-induced AP activity in C2C12 cells and had no effect on TCF transcriptional activity. *Dkk1*, *Sost*, *Fzd2*, and *Fzd4* were not affected by *ERα* deletion (Supplemental Figure 8C), excluding the possibility that the attenuation of Wnt signaling was secondary to upregulation of Wnt inhibitors.

ERα$^{f/f}$;Prx1-cre mice do not lose cortical bone after ovariectomy. In our previous work, *ERα* deletion from osteoclasts prevented ovariectomy-induced (OVX-induced) loss of cancellous, but not cortical, bone (7). We therefore investigated whether the ERα in cells of the osteoblast lineage could indirectly influence endocortical resorption. Acquisition of peak bone mass in both the *Prx1-cre* and *Col1a1-cre* strains occurred at approximately 16 weeks of age. Control and *ERα$^{f/f}$;Prx1-cre* mice were ovariectomized at 8 or 24 weeks of age, and the effects of the loss of estrogens were examined 3 and 6 weeks later, respectively. Mice ovariectomized at 8 weeks of age showed the expected loss of uterine weight (Supplemental Figure 9A). Littermate control mice exhibited decreased bone accrual at the spine and femur, as determined by DEXA BMD (Figure 7A). *ERα$^{f/f}$;Prx1-cre* mice also exhibited decreased bone accrual at the spine. In contrast, femoral DEXA BMD was unaltered in the ovariectomized *ERα$^{f/f}$;Prx1-cre* mice. Nonetheless, micro-CT analysis revealed that OVX did cause loss of cancellous bone accrual (Figure 7B), a decrease in trabecular number, and an increase in trabecular separation (Supplemental Figure 10A) in both the littermate controls and *ERα$^{f/f}$;Prx1-cre* mice. On the other hand, OVX caused a decrease in the accrual of cortical BMD in control but not in *ERα$^{f/f}$;Prx1-cre* mice (Figure 7C). In agreement with these findings, histomorphometric analysis of the endocortical surface of femoral bone sections revealed an increase in the number of osteoclasts in the *ERα$^{f/f}$* control mice following OVX (Figure 7D). This increase was abrogated in the *ERα$^{f/f}$;Prx1-cre* mice. Similar findings to those from the OVX experiment with 8-week-old (growing) mice were obtained in mice ovariectomized at 24 weeks of age (Figure 7E and Supplemental Figure 9B).

Consistent with the critical role of estrogens in epiphyseal closure at the end of puberty in humans as well as the fact that *Prx1-cre* is expressed in growth plate chondrocytes (Figure 1A and ref. 10), OVX

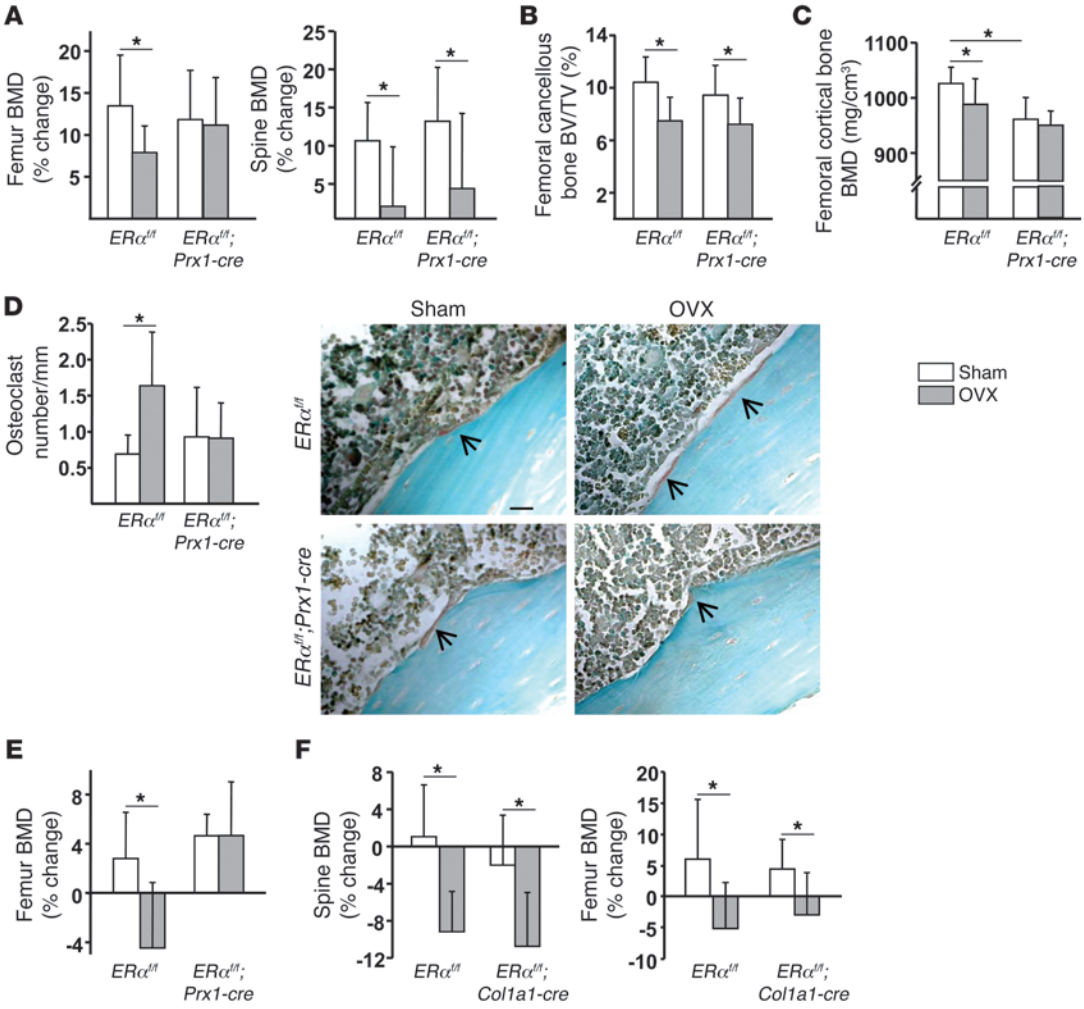

Figure 7

Cortical bone is preserved in *ERα$^{f/f}$;Prx1-cre* mice following OVX. (**A**–**D**) Eight-week-old female mice were sham operated or ovariectomized and euthanized 3 weeks later (n = 10/group). (**A**) The percentage of change from the initial BMD was determined by DEXA measurements 1 day before surgery and before death. (**B**) Cancellous bone mass and (**C**) BMD of cortical bone at the distal femur determined by micro-CT. (**D**) Osteoclast number per mm of endocortical bone surface in longitudinal decalcified sections of femurs (n = 10/group). In the photomicrographs, osteoclasts (stained red by TRAP; scale bar: 20 μm) are indicated by the arrows. (**E**) Twenty-two-week-old mice were sham operated or ovariectomized and euthanized 6 weeks later (n = 4–6/group). The percentage of change in BMD was determined as in **B**. (**F**) Twenty-week-old mice were sham operated or ovariectomized and euthanized 6 weeks later (n = 11/group). The percentage of change in BMD was determined as in **A**. Bars represent mean and SD. *P < 0.05 by 2-way ANOVA.

of 8-week-old mice with deletion of *ERα* from *Prx1-cre*–expressing cells did not cause an increase in bone length, which was readily seen in the ERα intact mice (Supplemental Figure 10B).

Last, in contrast to the *ERα$^{f/f}$;Prx1-cre* mice, *ERα$^{f/f}$;Col1a1-cre* mice ovariectomized at 20 week of age exhibited a similar loss of spinal and femoral BMD as that of their littermate controls 6 weeks following OVX (Figure 7F).

Discussion

The studies described herein reveal that the ERα present in cells of the osteoblastic lineage is required for optimal accrual and maintenance of cortical bone mass. Moreover, they show that these functions of the ERα are due to its activity in osteoblast progenitors but not in mature osteoblasts or osteocytes. Specifically, deletion of *ERα* from pluripotent mesenchymal progenitors, using *Prx1-cre*, or from osteoblast progenitors, using *Osx1-cre*, produced similar reductions in cortical bone mass, whereas deletion from more mature cells, using *Col1a1-cre*, had no impact on bone mass or architecture.

The effect of the osteoblast progenitor ERα on cortical bone mass evidently resulted from its ability to potentiate Wnt/TCF-mediated transcription and thereby promote the proliferation and differentiation of periosteal osteoblasts. This led to increased bone formation in the periosteal surface and thereby increased cortical thickness. In line with our findings, it is well established that Wnt signaling is a critical regulator of osteoblast supply and bone mass (19, 20). Canonical Wnt signaling stabilizes β-catenin, which binds to and activates members of the TCF/lymphoid enhancer factor transcription factor family (21). Through this mechanism, canonical Wnt/β-catenin signaling promotes the progression of

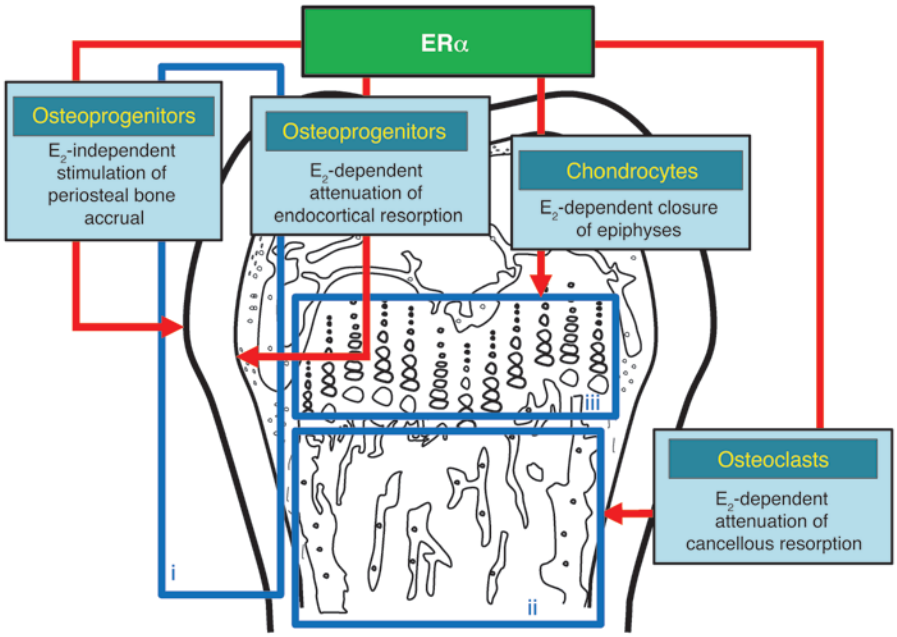

Figure 8
Site-specific effects of ERα on different bone compartments. (Box i) The cortical and (Box ii) the cancellous bone compartments as well as (Box iii) the growth plate of a long bone are depicted in the respective blue boxes. The cells responsible for the particular action along with their dependency or lack thereof on estrogens (E_2) in each compartment are deduced from the respective cell-specific ERα deletion murine models of the present work and two earlier papers in which ERα was selectively deleted in osteoclasts (7) and chondrocytes (48). Red arrows point to the site at which the effect summarized in the blue boxes occurs.

osteoblast progenitors expressing the *Osx1* gene to bone-producing osteoblasts (11). On the other hand, Wnt/β-catenin signaling is a potent suppressor of adipocyte differentiation (22). Consistent with this and evidence that *Osx1-cre* transgene is active in cells capable of becoming both osteoblasts and adipocytes (23), the number of adipocyte progenitors (CFU-AD) was increased in the mice lacking ERα in osteoblast progenitors.

Our results also suggest that the stimulatory effect of ERα on Wnt/β-catenin signaling and periosteal cell proliferation did not require activation of the receptor protein by estrogens. Thus, in the absence of estrogens, Wnt-induced proliferation and differentiation of osteoprogenitors was attenuated in periosteal- or bone marrow–derived osteoblastic cell cultures established from the femurs of mice with deletion of *ERα* from *Osx1-cre*–expressing cells as well as in an osteoblastic cell line in which the *ERα* was silenced. β-Catenin/TCF transcriptional activity was also attenuated in the latter cell model. In contrast, estradiol had either no effect or inhibited Wnt/β-catenin–induced proliferation and differentiation of osteoprogenitors in cell cultures from mice with intact *ERα*. Moreover, in agreement with earlier results of ours (15, 16), addition of 17β-estradiol to periosteal- or bone marrow–derived cell cultures from mice with intact *ERα* had an attenuating effect on osteoblastogenesis, demonstrating that the effects of the estrogen-activated ERα are opposite to the effects of the unliganded ERα. In full support of the contention that the unliganded ERα has a diametrically opposite effect to that of estrogens on periosteal bone expansion, it is documented that estrogens suppress periosteal bone formation and that estrogen deficiency in female rodents and women increases periosteal apposition (2, 24). Be that as it may, we cannot completely exclude the possibility that some residual estrogens in the charcoal-stripped serum or estrogens produced by osteoblasts themselves or perhaps estrogen-like alternative ligands could have activated the ERα (25, 26).

In line with our findings with the selective *ERα* deletion in osteoblast progenitors, periosteal bone formation in response to mechanical loading is abrogated in mice with global deletion of the *ERα* (27). Likewise, LDL receptor-related protein 5/Wnt/β-catenin signaling is a normal physiological response to mechanical loading, and activation of this pathway enhances the sensitivity of osteoblastic cells to mechanical loading (28–30). In vitro studies have suggested that activation of the Wnt/β-catenin pathway in response to mechanical stimulation requires the ERα (17). Furthermore, the effect of mechanical loading in mice is independent of the presence of estrogens (31, 32) and does not require the ligand-binding domain of ERα (33). It is, therefore, plausible that the cortical deficit in our studies was the result of a compromised response to mechanical loading.

Male mice with deletion of *ERα* from *Prx1-cre*–expressing cells had a similar phenotype to that of their female counterparts. These observations are in line with the evidence that systemic loss of *ERα* leads to lower cortical bone mass in male mice and men (34, 35). However, global deficiency of *ERα* can cause a loss of cortical bone mass as a result of increased resorption. Be that as it may, in contrast to that in the females, the cortical defect in male mice in our studies was transient, probably because androgens acting via the androgen receptor in males stimulate periosteal bone expansion (36–39). Hence, androgen actions in the male *ERα$^{f/f}$;Prx1-cre* mice must have countered the lack of ERα.

Deletion of the *ERα* from pluripotent mesenchymal cells expressing *Prx1-cre*, osteoblast precursors expressing *Osx1-cre*, or osteoblasts and osteocytes expressing *Col1a1-cre* had no effect on cancellous bone in either intact or ovariectomized animals. These findings are consistent with, and complement, our earlier work showing that the osteoclast *ERα* is responsible for the protective effects of estrogen on cancellous bone (7). In that earlier work with mice lacking *ERα* in the entire osteoclast lineage (LysM-expressing cells), cortical bone resorption was not affected, indicating that other cell types are the targets of the restraining effect of estrogens on the resorption of this compartment. In support of this, over the years, studies with cell models, primary cell cultures, and gonadectomized rodents have suggested that estrogens inhibit bone resorption by attenuating osteoclastogenic cytokine

production by osteoblast progenitors and that this results from the ability of estrogens to inhibit NF-κB (4, 40). In agreement with this evidence, we found here that mice lacking *ER*α in osteoblast progenitors not only had low cortical bone at baseline because of the lack of the anabolic effect of the unliganded ERα in the periosteum, but, unlike their littermate controls, did not exhibit increased osteoclast numbers in the endocortical surface and loss of endocortical bone mass following OVX. This result strongly suggests that the derepression of osteoclastogenic cytokine production and the increased osteoclastogenesis seen in the *ER*α-sufficient mice following loss of estrogens did not happen in the mice lacking *ER*α in osteoblast progenitors because there was no repression in the first place. In other words, loss of estrogens could not be perceived by cells lacking the *ER*α. Thus, the deletion of the *ER*α in the *Prx1-cre*–expressing cells reveals that estrogens acting via the ERα expressed in osteoblast progenitors exert a protective effect against osteoclastic resorption in the endocortical surface. Loss of this particular effect of estrogens following OVX must, therefore, be responsible for the loss of endocortical bone mass that occurred in the mice with intact *ER*α. Albeit, *ER*α deletion from *Prx1-cre*–expressing cells had no effect on endocortical resorption in the estrogen-replete state (nonovariectomized mice). The simplest explanation for this finding is that, in osteoblast progenitors lacking *ER*α (and therefore the inhibitory effect of estrogens) since conception, cytokine production and excessive osteoclastogenesis were restrained by compensatory cell autonomous means. Alternatively, osteocytes and/or other cells comprising the "mechanostat" might have sensed the low cortical thickness of the *ER*α-deficient mice and in response produced signals that countered "inappropriate" osteoclastogenesis and/or the recruitment of osteoclasts to the endocortical surface in an attempt to compensate for the loss of cortical bone.

Finally, in this work, we found that *ER*α deletion from mature osteoblasts increased the prevalence of apoptosis but had no effect on bone mass. This finding suggests that shortening the life span of mature osteoblasts in and of itself may not lead to discernible loss of bone mass unless it is accompanied by decreased osteoblastogenesis (as in the setting of aging) and/or increased osteoclastic bone resorption (as in the acute phase of estrogen deficiency).

In closing, our studies reveal that the ERα plays essential roles in the accumulation and maintenance of bone mass via cell-autonomous actions in both osteoblast progenitors and osteoclasts (Figure 8). However, the role of ERα in these two cell types is different in distinct bone compartments: the ERα in osteoblast progenitors promotes bone formation at the periosteal surface of the cortex and prevents resorption at the endocortical surface, whereas the ERα in osteoclasts prevents resorption of cancellous bone. The role of ERα in osteoblast progenitors is further characterized by both ligand-mediated and ligand-independent actions. The latter is likely important for the increased bone formation in response to strains from surrounding tissues and gravity and thus the mechanical adaptation of the skeleton.

Methods

Animal experimentation. To disrupt the *ER*α gene at different stages of the osteoblast lineage, *ERα*$^{f/f}$ mice (7) were crossed with mice expressing the *Prx1-cre* (9), *Osx1-cre* (11), and *Col1a1-cre* transgenes (14). The experimental mice were generated using a 2-step breeding strategy. Hemizygous Cre transgenic mice were crossed with homozygous *ERα*$^{f/f}$ mice to generate heterozygous *ERα*$^{f/+}$ offspring, with and without a cre allele. These offspring were then intercrossed to generate the following: wild-type mice, mice hemizygous for a cre allele, mice homozygous for the *ERα*$^{f/f}$ allele, and *ERα*$^{f/f}$ mice that were also hemizygous for a cre allele. Offspring were genotyped by PCR using the following primer sequences: Cre forward, 5′-GCGGTCTGGCAGTAAAAACTATC-3′, Cre reverse, 5′-GTGAAACAGCATTGCTGTCACTT-3′ (product size 102 bp); *ERα*$^{f/f}$ forward, 5′-TCGTTTTGAATTAATTATGAATGTCTG-3′, *ERα*$^{f/f}$ reverse, 5′-TTCATGTGTTGTGCAAATAGC-3′ (product size 647 bp [WT] and 933 bp [floxed allele]).

Eight-week-old female *ERα*$^{f/f}$*;Prx1-cre* mice and their *ERα*$^{f/f}$ littermates were sham operated or ovariectomized. After 3 weeks, animals were sacrificed, and the tissues were dissected for further analyses. BMD measurements were performed 1 day prior to surgery and before sacrifice. OVX or sham operations were also performed in 22-week-old *ERα*$^{f/f}$*;Prx1-cre* and 20-week-old *ERα*$^{f/f}$*;Col1a1-cre* mice and respective littermate controls, and the mice were sacrificed 6 weeks later. Mice were injected with tetracycline 6 and 2 days before harvesting.

Bone imaging. BMD measurements were performed by DEXA using a PIXImus densitometer (GE Lunar), as previously described (41), in mice sedated with 2% isoflurane. The spine window was a rectangle depending on animal body length, reaching from just below the skull to the base of the tail. The femoral window captured the entire left femur. Micro-CT analysis was done after the bones were dissected, cleaned, fixed in 10% Millonig's formalin and transferred to 100% ethanol, loaded into 10-mm diameter scanning tubes, and imaged (μCT40, Scanco Medical), and the vertebral and femoral cancellous bone was analyzed as previously described (42). Transverse CT slices (n = 61) were also acquired at the vertebrae to assess cortical thickness. At medium resolution (nominal isotropic voxel size = 12 μm), 550 slices were acquired and 400 were used for analysis. Scans were integrated into 3D voxel images (1,024 × 1,024 pixel matrices for each individual planar stack). A Gaussian filter (sigma = 0.8, support = 1) was applied to all analyzed scans. Key parameters were as follows: x-ray tube potential = 55 kVp, x-ray intensity = 145 μA, integration time = 200 ms, and threshold = 200 mg/cm^3. Image processing language scripts, including the "cl_image" command, were used to obtain the femoral endocortical and periosteal circumference. Micro-CT measurements were expressed in 3D nomenclature. After a 1-hour warm-up period, calibration and quality control were done weekly using 5 density standards, and spatial resolution was verified monthly using a tungsten wire rod. Beam-hardening correction was based on the calibration records. Corrections were made for 200 mg/cm^3 hydroxyapatite for all energies. Over the past 3 years, the coefficient of variation for the fifth density standard (mean 5) was 0.97% (787 ± 7.6 SD mg HA/cm^3) and for rod volume was 2.18% (0.0642 ± 0.0014 SD cm^3).

Histology. Femurs were fixed in 10% Millonig's formalin, transferred to 100% ethanol, and embedded undecalcified in methyl methacrylate. The histomorphometric examination was performed in longitudinal sections using the OsteoMeasure Analysis System (OsteoMetrics Inc.). Static histomorphometry measurements of the cancellous bone were restricted to the secondary spongiosa. Endocortical and periosteal bone formation analyses were limited to femoral diaphysis and performed as described above. The following dynamic measurements were made: total perimeter (B.Pm); single label perimeter (sL.Pm); double label perimeter (dL.Pm), and MAR. The following values were then calculated: percentage MS/bone surface (%MS/BS) = ([1/2 sL.Pm + dL.Pm]/B.Pm × 100) and BFR/BS (μm^2/μm/d) = MAR × MS/BS. To visualize endocortical osteoclasts, additional femurs were decalcified with 14% EDTA and embedded in paraffin. Analyses were performed on tartrate resistant acid phosphatase–stained (TRAP-stained), femoral longitudinal, 5-μm-thick sections from the midshaft up to 2.5 mm toward the distal end. Approximately 10–20 osteoclasts were counted over 11.23 ± 1.5 mm of the endocortical perimeter. Cartilage was visualized by Safranine O staining on paraffin sections.

Cell culture. CFU-F, CFU-AD, and CFU-OB number was determined as previously described (15), using guinea pig feeder cells (43), 15% FBS, and 1 mM ascorbate-2-phosphate. Half of the medium was replaced every 5 days. CFU-Fs were enumerated at 10 days of culture after staining for AP, and CFU-OBs were enumerated at 25 days of culture after von Kossa staining. CFU-AD was enumerated at 6 days of culture in presence of 1 μM rosiglitazone after Oil-Red O staining.

Mineralization and other assays. To obtain periosteal cells, femurs and tibias isolated from 3- to 5-week-old mice were dissected free of muscle and connective tissue under sterile conditions. Periosteal tissue was dissected from the proximal end with a scalpel and placed in α-MEM containing 10% FBS until it reached 90% confluence. Half of the medium was replaced every 5 days. For experiments, periosteal or murine bone marrow cells pooled from 3 mice of each genotype were seeded on 12-well tissue culture plates at 5×10^6 cells per well in standard culture medium. After 10 days of culture, serum was changed to 2% charcoal-striped FBS and 50 ng/ml BMP-2 or ascorbic acid was added in the presence of vehicle or 10^{-8} M E_2. Two days later, 10 mM β-glycerolphosphate was added to the medium. The mineralized matrix was stained with 40 mM alizarin red solution after 2 weeks. Osteocalcin in the medium was quantified using an ELISA Kit (Biomedical Technologies Inc.). BrdU incorporation was measured with a Cell Proliferation ELISA Chemiluminescence Kit (Roche Diagnostics). Caspase-3 activity was quantified by determining the degradation of the fluorometric substrate DEVD (Biomol Research Labs), and protein concentration was measured using a Bio-Rad detergent-compatible kit (Bio-Rad DC Protein Assay Kit), as described previously (44). AP activity was determined in cells cultured for 7 days in 10% charcoal-striped FBS and lysed in 100 mM glycine, 1 mM $MgCl_2$, and 1 % Triton X-100 at pH 10 using a buffer containing 2-amino-2-methylpropanol and p-nitrophenylphosphate (Sigma-Aldrich). AP activity was normalized to total protein concentration, determined as above.

Isolation of Osx1-GFP cells. Calvaria cells were isolated from 3- to 4-day-old *Osx1-Cre*$^+$ mice bearing either the wild-type or *ERα*$^{f/f}$ alleles, as described previously (45), and cultured in T175 flasks in the presence of 1% ascorbic acid. At approximately 80% confluence, cells were trypsinized and the GFP-positive cells were sorted using a BD FACS Aria Cell Sorter (BD Biosciences). The GFP-positive cells were cultured in a 6-well plate until 90% confluence and harvested for RNA isolation.

Quantitative PCR. Soft tissues were removed from mice and immediately stored in liquid nitrogen. Osteocyte-enriched bone was obtained by removing the ends of femurs and tibias and flushing the bone marrow with PBS, followed by collagenase digestions, as previously described (10). Total RNA was extracted from tissues or cultured cells using Ultraspec (Biotecx Laboratories) and reverse-transcribed using the High-Capacity cDNA Archive Kit (Applied Biosystems), according to the manufacturer's instructions. TaqMan quantitative PCR was performed as previously described (46) to determine mRNA levels using the following primers manufactured by the TaqMan Gene Expression Assays service (Applied Biosystems): Mm00433148_mH (ERα), Mm00501578_m1 (Runx2), Mm00801666_g1 (Col1a1), and Mm00475528_m1 (ribosomal protein S2). Osx1 and Bglap were quantified using the custom-made TaqMan Assay-by-Design primer sets, 5′ATCTGACTTTGCTCCCCTTAACC3′, 5′GGGCCCTGGTTGCAAGA3′ and 5′GCTGCGCTCTGTCTCTCTGA3′, 5′TGCTTGGACATGAAGGCTTTG3′, respectively. mRNA expression levels were normalized to the house-keeping gene ribosomal protein S2 using the ΔCt method (47).

Genomic DNA was isolated from decalcified bone fragments after digestion with proteinase K and phenol/chloroform extraction. The efficiency of ERα genomic deletion was quantified using the TaqMan Assay-by-Design primer set 5′AGCAGTAACGAGAAAGGAAACATGA3′, 5′CATTGCACACGGCACAGTAG3′.

Silencing and transfection studies. C2C12 cells were cultured in DMEM supplemented with 10% FBS; 1% each penicillin, streptomycin, and glutamine; and 1% sodium pyruvate. Expression of ERα was knocked down by transduction with lentiviruses encoding shRNA to ERα (NM_007956) according to the manufacturer protocol. C2C12 cells transduced with a nontarget shRNA (SHC002V) were used as control. The silenced cells were selected with puromycin (2,500 ng/ml) for 14 days. The TCF-luc plasmid construct was introduced into C2C12 cells and cultured in 48-well plates by transient transfection using Lipofectamine Plus (Invitrogen). Luciferase activity was quantified using the Dual-Luciferase Reporter Assay System (Promega), according to the manufacturer's instructions. Light intensity was measured with a luminometer and normalized to Renilla-luc values for transfection efficiency.

Statistics. Group mean values were compared, as appropriate, by Student's unpaired 2-tailed *t* test and 1-way or 2-way ANOVA with Bonferroni's multiple comparison test, after determining that the data were normally distributed and exhibited equivalent variances. A P value ≤ 0.05 was considered significant.

Study approval. Procedures were approved by Institutional Animal Care and Use Committees of the University of Arkansas for Medical Sciences and the Central Arkansas Veterans Healthcare System.

Acknowledgments

This work was supported by the NIH (P01 AG13918, R01 AR56679, and R01 AR49794); the Department of Veterans Affairs from the Biomedical Laboratory Research and Development Service of the VA Office of Research and Development to R.L. Jilka (I01 BX000514), R.S. Weinstein (I01 BX000436), C.A. O'Brien (I01 BX000294), and S.C. Manolagas (I01 BX001405); and the University of Arkansas for Medical Sciences Translational Research Institute and Tobacco Settlement Funds. M. Martin-Millan was the recipient of an award from Marques de Valdecilla Foundation, Santander, Spain. E. Ambrogini was supported by a fellowship from the University of Pisa, Italy. We thank A. Warren, J. Crawford, R. Shelton, A. DeLoose, E. Hogan, and S. Berryhill for technical assistance; L. Elrod for help with the preparation of the manuscript; and H. Zhao and M. Parfitt for reviewing the manuscript.

Received for publication July 20, 2012, and accepted in revised form October 11, 2012.

Address correspondence to: Stavros C. Manolagas, 4301 West Markham, #587, Little Rock, Arkansas 72205-7199, USA. Phone: 501.686.5130; Fax: 501.686.8148; E-mail: manolagasstavros@uams.edu.

Marta Martin-Millan's present address is: Department of Internal Medicine, Hospital U. M. Valdecilla, University of Cantabria, Santander, Spain.

Melda Onal's present address is: Department of Biochemistry, University of Wisconsin-Madison, Madison, Wisconsin, USA.

1. Seeman E. Modeling and remodeling. In: Bilezikian JP, Raisz LG, Martin TJ, eds. *Principles of Bone Biology*. 3rd ed. San Diego, California, USA: Academic Press; 2008:3–28.
2. Seeman E. Periosteal bone formation--a neglected determinant of bone strength. *N Engl J Med*. 2003;349(4):320–323.
3. Perry RJ, Farquharson C, Ahmed SF. The role of sex steroids in controlling pubertal growth. *Clin Endocrinol (Oxf)*. 2008;68(1):4–15.
4. Manolagas SC. Birth and death of bone cells: basic regulatory mechanisms and implications for

the pathogenesis and treatment of osteoporosis. *Endocr Rev*. 2000;21(2):115–137.
5. Manolagas SC. From estrogen-centric to aging and oxidative stress: a revised perspective of the pathogenesis of osteoporosis. *Endocr Rev*. 2010;31(3):266–300.
6. Riggs BL, Khosla S, Melton LJ III. Sex steroids and the construction and conservation of the adult skeleton. *Endocr Rev*. 2002;23(3):279–302.
7. Martin-Millan M, et al. The estrogen receptor alpha in osteoclasts mediates the protective effects of estrogens on cancellous but not cortical bone. *Mol Endocrinol*. 2010;24(2):323–334.
8. Nakamura T, et al. Estrogen prevents bone loss via estrogen receptor alpha and induction of Fas ligand in osteoclasts. *Cell*. 2007;130(5):811–823.
9. Logan M, Martin JF, Nagy A, Lobe C, Olson EN, Tabin CJ. Expression of Cre Recombinase in the developing mouse limb bud driven by a Prxl enhancer. *Genesis*. 2002;33(2):77–80.
10. Xiong J, Onal M, Jilka RL, Weinstein RS, O'Brien CA. Matrix-embedded cells control osteoclast formation. *Nat Med*. 2011;17(10):1235–1241.
11. Rodda SJ, McMahon AP. Distinct roles for Hedgehog and canonical Wnt signaling in specification, differentiation and maintenance of osteoblast progenitors. *Development*. 2006;133(16):3231–3244.
12. Maes C, et al. Osteoblast precursors, but not mature osteoblasts, move into developing and fractured bones along with invading blood vessels. *Dev Cell*. 2010;19(2):329–344.
13. Davey RA, et al. Decreased body weight in young Osterix-Cre transgenic mice results in delayed cortical bone expansion and accrual. *Transgenic Res*. 2011;21(4):885–893.
14. Dacquin R, Starbuck M, Schinke T, Karsenty G. Mouse alpha1(I)-collagen promoter is the best known promoter to drive efficient Cre recombinase expression in osteoblast. *Dev Dyn*. 2002;224(2):245–251.
15. DiGregorio G, et al. Attenuation of the self-renewal of transit amplifying osteoblast progenitors in the murine bone marrow by 17β-estradiol. *J Clin Invest*. 2001;107(7):803–812.
16. Almeida M, et al. Estrogens attenuate oxidative stress, osteoblast differentiation and apoptosis by DNA binding-independent actions of the ERalpha. *J Bone Mineral Res*. 2010;25(4):769–781.
17. Armstrong VJ, et al. Wnt/beta-catenin signaling is a component of osteoblastic bone cell early responses to load-bearing and requires estrogen receptor alpha. *J Biol Chem*. 2007;282(28):20715–20727.
18. Sunters A, et al. Mechano-transduction in osteoblastic cells involves strain-regulated estrogen receptor alpha-mediated control of insulin-like growth factor (IGF) I receptor sensitivity to ambient IGF, leading to phosphatidylinositol 3-kinase/AKT-dependent Wnt/LRP5 receptor-independent activation of beta-catenin signaling. *J Biol Chem*. 2010;285(12):8743–8758.
19. Almeida M, Han L, Martin-Millan M, O'Brien CA, Manolagas SC. Oxidative stress antagonizes Wnt signaling in osteoblast precursors by diverting beta-catenin from T cell factor- to forkhead box O-mediated transcription. *J Biol Chem*. 2007; 282(37):27298–27305.
20. Almeida M, Ambrogini E, Han L, Manolagas SC, Jilka RL. Increased lipid oxidation causes oxidative stress, increased PPAR{gamma} expression and diminished pro-osteogenic Wnt signaling in the skeleton. *J Biol Chem*. 2009;284(40):27438–27448.
21. Bienz M, Clevers H. Armadillo/beta-catenin signals in the nucleus — proof beyond a reasonable doubt? *Nat Cell Biol*. 2003;5(3):179–182.
22. Prestwich TC, MacDougald OA. Wnt/beta-catenin signaling in adipogenesis and metabolism. *Curr Opin Cell Biol*. 2007;19(6):612–617.
23. Song L, Liu M, Ono N, Bringhurst FR, Kronenberg HM, Guo J. Loss of wnt/beta-catenin signaling causes cell fate shift of preosteoblasts from osteoblasts to adipocytes. *J Bone Miner Res*. 2012; 27(11):2344–2358.
24. Callewaert F, Sinnesael M, Gielen E, Boonen S, Vanderschueren D. Skeletal sexual dimorphism: relative contribution of sex steroids, GH-IGF1, and mechanical loading. *J Endocrinol*. 2010; 207(2):127–134.
25. McCarthy TL, Clough ME, Gundberg CM, Centrella M. Expression of an estrogen receptor agonist in differentiating osteoblast cultures. *Proc Natl Acad Sci U S A*. 2008;105(19):7022–7027.
26. Umetani M, et al. 27-Hydroxycholesterol is an endogenous SERM that inhibits the cardiovascular effects of estrogen. *Nat Med*. 2007;13(10):1185–1192.
27. Lee K, Jessop H, Suswillo R, Zaman G, Lanyon L. Endocrinology: bone adaptation requires oestrogen receptor-alpha. *Nature*. 2003;424(6947):389.
28. Robinson JA, et al. Wnt/beta-catenin signaling is a normal physiological response to mechanical loading in bone. *J Biol Chem*. 2006;281(42):31720–31728.
29. Tu X, et al. Sost downregulation and local Wnt signaling are required for the osteogenic response to mechanical loading. *Bone*. 2012;50(1):209–217.
30. Sawakami K, et al. The Wnt co-receptor LRP5 is essential for skeletal mechanotransduction but not for the anabolic bone response to parathyroid hormone treatment. *J Biol Chem*. 2006;281(33):23698–23711.
31. Sugiyama T, Galea GL, Lanyon LE, Price JS. Mechanical loading-related bone gain is enhanced by tamoxifen but unaffected by fulvestrant in female mice. *Endocrinology*. 2010;151(12):5582–5590.
32. Hagino H, Raab DM, Kimmel DB, Akhter MP, Recker RR. Effect of ovariectomy on bone response to in vivo external loading. *J Bone Miner Res*. 1993; 8(3):347–357.
33. Windahl SH, et al. Estrogen receptor alpha amplifies the osteogenic response to mechanical loading in a ligand-independent manner by its activation function 1 but not 2 [Abstract]. *Bone*. 2012;50(S1):S50.
34. Sims NA, et al. Deletion of estrogen receptors reveals a regulatory role for estrogen receptors-beta in bone remodeling in females but not in males. *Bone*. 2002;30(1):18–25.
35. Smith EP, et al. Estrogen resistance caused by a mutation in the estrogen-receptor gene in a man. *N Engl J Med*. 1994;331(16):1056–1061.
36. Bouillon R, Bex M, Vanderschueren D, Boonen S. Estrogens are essential for male pubertal periosteal bone expansion. *J Clin Endocrinol Metab*. 2004; 89(12):6025–6029.
37. Callewaert F, Boonen S, Vanderschueren D. Sex steroids and the male skeleton: a tale of two hormones. *Trends Endocrinol Metab*. 2010;21(2):89–95.
38. Windahl SH, et al. Reduced bone mass and muscle strength in male 5alpha-reductase type 1 inactivated mice. *PLoS One*. 2011;6(6):e21402.
39. Callewaert F, et al. Differential regulation of bone and body composition in male mice with combined inactivation of androgen and estrogen receptor-alpha. *FASEB J*. 2009;23(1):232–240.
40. Manolagas SC, Jilka RL. Bone marrow, cytokines, and bone remodeling — Emerging insights into the pathophysiology of osteoporosis. *N Engl J Med*. 1995;332(5):305–311.
41. O'Brien CA, Jilka RL, Fu Q, Stewart S, Weinstein RS, Manolagas SC. IL-6 is not required for parathyroid hormone stimulation of RANKL expression, osteoclast formation, and bone loss in mice. *Am J Physiol Endocrinol Metab*. 2005;289(5):E784–E793.
42. Jilka RL, et al. Decreased oxidative stress and greater bone anabolism in the aged, as compared to the young, murine skeleton by parathyroid hormone. *Aging Cell*. 2010;9(5):851–867.
43. Kuznetsov S, Robey PG. Species differences in growth requirements for bone marrow stromal fibroblast colony formation *in vitro*. *Calcif Tissue Int*. 1996;59(4):265–270.
44. Plotkin LI, Weinstein RS, Parfitt AM, Roberson PK, Manolagas SC, Bellido T. Prevention of osteocyte and osteoblast apoptosis by bisphosphonates and calcitonin. *J Clin Invest*. 1999;104(10):1363–1374.
45. Jilka RL, Weinstein RS, Bellido T, Parfitt AM, Manolagas SC. Osteoblast programmed cell death (apoptosis): modulation by growth factors and cytokines. *J Bone Miner Res*. 1998;13(5):793–802.
46. Almeida M, Han L, Bellido T, Manolagas SC, Kousteni S. Wnt proteins prevent apoptosis of both uncommitted osteoblast progenitors and differentiated osteoblasts by beta-catenin-dependent and -independent signaling cascades involving Src/ERK and phosphatidylinositol 3-kinase/AKT. *J Biol Chem*. 2005;280(50):41342–41351.
47. Livak KJ, Schmittgen TD. Analysis of relative gene expression data using real-time quantitative PCR and the 2(-Delta Delta C(T)) Method. *Methods*. 2001;25(4):402–408.
48. Borjesson AE, et al. The role of estrogen receptor alpha in growth plate cartilage for longitudinal bone growth. *J Bone Miner Res*. 2010;25(12):2690–2700.